Novel multi-transmitter calyx-like giant synapse revealed in the extended amygdala

Limei Zhang[1, 2†,10*], Vito S. Hernández[1, 2†,10], David M. Giraldo[3, 4], Juan C. León-Contreras[5], Rong Ye[6], Shiliang Zhang[6], Martin K-H Schäfer[7], Rafael A. Barrio[8], Rogelio Hernández-Pando[5], Francesco Ferraguti[9] and Lee E. Eiden[2]

[1]Department of Physiology, School of Medicine, National Autonomous University of Mexico
[2]Section on Molecular Neuroscience, National Institute of Mental Health, NIH, USA.
[3]Microscopy Core, School of Medicine, National Autonomous University of Mexico, Mexico City Mexico.
[4] ZEISS Innovation Center, Carl Zeiss Microscopy, LLC, Dublin, California, USA
[5]Department of Experimental Pathology, National Institute of Medical Sciences and Nutrition, Mexico
[6]Confocal and Electron Microscopy Core, National Institute on Drug Abuse, NIH, USA.
[7]Center for Mind, Brain and Behavior, Philipps University of Marburg, Germany.
[8]Department of Complex Systems, Institute of Physics, UNAM, Mexico.
[9]Institute of Pharmacology, Medical University of Innsbruck, Innsbruck, Austria.
[10]Equal contribution
[†]Sabbatical researcher
*Correspondence: limei@unam.mx

Abstract: The calyx of Held is a giant excitatory cup-like axo-somatic synapse in the auditory brainstem and the only synapse of its kind described in the central nervous system.. Here, using PACAP immunohistochemistry combined with confocal and tomographic electron microscopy, we report the discovery of a morphologically similar calyx-like synapse in the extended amygdala of rodents that exhibits unique neurochemical features. This previously unrecognized structure forms enveloping axo-somatic terminals with mixed glutamatergic and cholinergic identities, co-expressing VGluT1, VGluT2, VAChT, and the neuropeptides PACAP, CGRP, and neurotensin, along with calretinin in the presynaptic compartment. The postsynaptic targets are a distinct subset of PKCd-expressing neurons that co-express the synaptic adhesion molecule GluD1. Strikingly, GluD1 immunolabeling is concentrated specifically at axo-somatic contact sites apposed to VAChT+ synaptic specifications, but absent at PSD of conventional type I synaptic specifications, within calyceal terminals, suggesting a specialized molecular architecture for them. Our findings reveal a previously unknown calyx-like synapse in the forebrain, exhibiting a unique convergence of fast and modulatory transmission with implications for transmission fidelity within an emotional-viscerosensory circuit.

Significance Statement: Fast and reliable excitatory transmission is essential for neural circuits for rapid sensory processing. Until now, the calyx of Held synapse was the only known giant axo-somatic glutamatergic terminal in the mammalian brain. Here, we identify a previously unrecognized calyx-like synapse in the extended amygdala, a center for emotional and autonomic integration. This massive, multimodal synapse combines glutamatergic, cholinergic, and peptidergic transmission and targets a distinct subset of PKCd neurons. Its molecular composition, including VGluT1/2, VAChT, neuropeptides including PACAP, NTs and CGRP, and GluD1 suggests a unique structural and functional specialization. This discovery broadens our understanding of synaptic diversity and reveals a novel anatomical substrate for high-fidelity communication in emotional-viscerosensory circuits.

Key words: Calyx of Held, axo-somatic synapse, FEBSEM, TEM, multi-transmitters, co-transmission, neuropeptides, GluD1, PKCd

Introduction

Precise and high-fidelity neurotransmission is a hallmark of certain specialized synaptic architectures in the mammalian brain. One of the most striking examples is the calyx of Held, a giant axo-somatic glutamatergic terminal in the auditory brainstem (Nakamura and Cramer 2011), first described over a century ago by Hans Held (Held 1893). This unique synapse, formed by globular bushy cells onto principal neurons in the medial nucleus of the trapezoid body (MNTB), is characterized by its expansive presynaptic terminal that engulfs the soma of its postsynaptic target, supporting fast, one-to-one spike transmission with minimal delay and jitter (Satzler, Sohl et al. 2002, Lorteije, Rusu et al. 2009, Nakamura and Cramer 2011). The structure and function of the calyx of Held have provided a foundational model for understanding synaptic reliability, vesicle dynamics, and temporal precision in sensory circuits.

While previous studies have noted that some features of calyx synapses can be observed in hippocampal mossy fiber boutons and cerebellar climbing fiber terminals (Harris and Weinberg 2012), these structures predominantly target dendrites and do not fully recapitulate the enveloping, axo-somatic morphology characteristic of the calyx of Held. Similarly, earlier reports describing basket-like axosomatic contacts formed by neuropeptide calcitonin gene-related peptide (CGRP) (Schwaber, Sternini et al. 1988, Gandhi, Gawande et al. 2021) (Shimada, Shiosaka et al. 1985), pituitary adenylate cyclase activating polypeptide (PACAP) (Missig, Roman et al. 2014), neurotensin (Torruella-Suarez, Vandenberg et al. 2020) and forming type II axo-somatic synapses under transmission electron microscopy (Shimada, Shiosaka et al. 1985, Takeuchi, Xie et al. 2004, Dong, Fukazawa et al. 2010), have not demonstrated that these terminals engulf their postsynaptic targets. Therefore, to our knowledge, a fully enveloping calyx-like fast relay synapse has not yet been described in forebrain circuits.

The central amygdala (CeA) and bed nucleus of the stria terminalis (BST) serve as crucial hubs for rapid viscerosensory processing and for coordinating autonomic, behavioral, and emotional responses to threats and homeostatic challenges (Goehler 2011). These interconnected nuclei receive robust brainstem inputs carrying visceral and nociceptive information – notably from the parabrachial nucleus (PBN) – which alert the extended amygdala to internal bodily states and imminent threats (Takeuchi, Xie et al. 2004, Jaramillo, Brown et al. 2021). In turn, the CeA and BST project to hypothalamic and brainstem effectors to orchestrate fear and stress responses. For example, the CeA is well known to drive defensive behaviors (like freezing and startle) and autonomic adjustments (such as changes in heart rate and stress hormone release) during conditioned fear, via its projections to the brainstem and hypothalamus (Radke 2009).

In the course of characterizing the distribution of pituitary adenylate cyclase activating polypeptide (PACAP)-containing fibers throughout the rodent brain, we serendipitously observed ring-like axo-somatic structures that appeared selectively in the capsular subdivision of the central amygdala (CeC) and in the oval nucleus of the bed nucleus of the stria terminalis (ovBST), with a more modest presence in the lateral septal nuclei. These structures, revealed by immunohistochemistry for PACAP, exhibited a morphology reminiscent of the calyx of Held. Using a combination of confocal microscopy, electron tomography (focused ion beam scanning electron microscopy, FIBSEM), and 3D reconstructions, we report here that these are indeed massive calyx-like terminals forming multiple synaptic contacts on the soma of a distinct protein kinase C d (PKCd) expressing

neuronal sub-population. Remarkably, the terminals exhibit a multimodal transmitter identity, co-expressing the vesicular glutamate transporter 1 and/or 2 (VGluT1 and/or VGluT2), vesicular acetylcholine transporter (VAChT), along with the neuropeptides PACAP, CGRP and neurotensin, as well as the calcium binding protein calretinin. Their postsynaptic targets besides PKCd, express GluD1, a synaptic adhesion molecule previously implicated in the stabilization of large glutamatergic synapses (Dai, Patzke et al. 2021, Liakath-Ali, Polepalli et al. 2022), suggesting the integration of excitatory, cholinergic, and peptidergic signaling at this site. Collectively, our findings uncover previously unknown calyx-like synapses in the forebrain, exhibiting a unique convergence of fast and modulatory transmission, with implications for the structural logic of high-fidelity signal integration in viscerosensory-affective circuits.

Results

PACAP-Containing ring-like structures identified in the Forebrain. To assess the distribution of PACAP containing inputs in the rodent telencephalon, we performed immunohistochemistry and identified a highly selective ring-like innervation pattern in distinct forebrain regions. These perisomatic PACAP-positive structures were especially prominent in the central amygdala, the capsular subdivision (CeC), the oval nucleus of the bed nucleus of stria terminalis (ovBST), and, to a lesser extent, scattered within the dorsal and ventral subdivisions of the lateral septal nucleus (see Supplemental Fig. 1). Within the amygdaloid complex (Fig. 1A–B), we observed heterogeneous PACAP immunoreactivity across multiple nuclei. A dense mesh of fine, varicose PACAP-immunoreactive (PACAP-ir) fibers was distributed in regions such as the lateral amygdala (LA, Fig. 1, A and B, B2), postero-dorsal medial amygdala (MePD, Fig. 1, A and B, and B4), posteroventral medial amygdala (MePV), basolateral (BLA), and basomedial (BMA, Fig. 1, A and B, B3) amygdala, as well as in the central lateral (CeL) and central medial (CeM) subdivisions (fig. 1, A and B, B3) forming diffuse *en passant* type innervation patterns. In contrast, the CeC displayed a population of thicker, non-varicose PACAP+ fibers forming distinct ring-like axo-somatic arrangements around a subpopulation of neurons (Fig. 1, A and B, B1, arrows).

Neuroanatomical Characterization of PACAP+ Calyceal Terminals. To determine the postsynaptic target of these PACAP containing rings, we first assessed somatostatin (SST)-expressing neurons, but these lacked expression of the PAC1 receptor. Since both the CeC and ovBST are known to also contain a high density of PKCd-expressing neurons (Botta, Demmou et al. 2015, Daniel and Rainnie 2016), we assessed this population mainly used a Prkcd-Cre::Ai9 double transgenic mice, in which PKCd-+ neurons are fluorescently labeled with TdTomato. Here, we detail the distinct morphological features of the PACAP-immunoreactive axonal terminals in the CeC, particularly enriched in its postero-ventro-lateral region (Fig. 1 C). These terminals display a perisomatic “calyx-like” arrangement, as seen in high-magnification confocal images (Fig. 1C1), and juxtapose with GluD1-immunolabeled domains of PKCd expressing neurons, supporting a direct axo-somatic PACAP containing input onto PKCδ+/GluD1+ neurons.

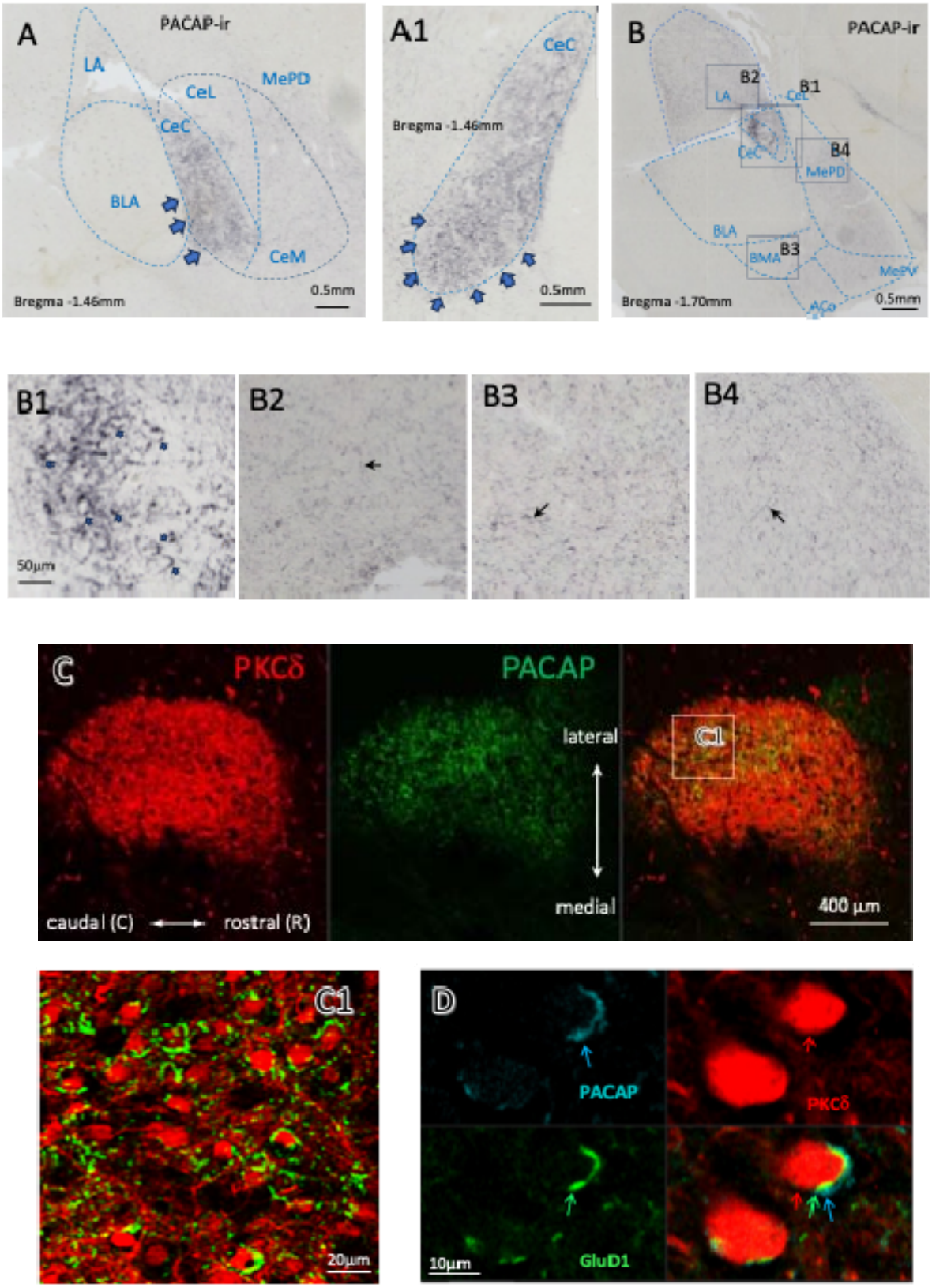
A
PACAP-ir
LA
MePD
CeL
CeC
BLA
CeM
Bregma -1.46mm
0.5mm
A1
CeC
Bregma -1.46mm
0.5mm
B
PACAP-ir
B2
B1
LA
CeL
CeC
B4
MePD
BLA
BMA
B3
MePV
ACo
Bregma -1.70mm
0.5mm
B1
50µm
B2
B3
B4
C
PKCδ
PACAP
lateral
medial
C1
caudal (C)
rostral (R)
400 µm
C1
20µm
D
PACAP
PKCδ
GluD1
10µm

Figure 1. PACAP immunopositive fibers form perisomatic ring-like innervation patterns targeting PKCδ neurons in the capsular division of the central amygdala (CeC). (A–B) Coronal sections of the rat amygdaloid complex immunostained for PACAP (PACAP-ir). Blue dashed outlines indicate subdivisions of the amygdaloid nuclei, including CeC (capsular), CeL (lateral), CeM (medial), BLA (basolateral), BMA (basomedial), LA (lateral), and MePD/MePV (posterodorsal/posteroventral medial amygdala). (A, A1) Contralateral amygdaloid complex at approximately bregma −1.46 mm. Blue-black arrowheads highlight ring-like PACAP-ir structures predominantly in the ventral portion of the CeC. (B) Amygdaloid complex at bregma −1.70 mm, where ring-like PACAP+ structures are observed exclusively in the CeC. (B1) Higher magnification of the boxed CeC region in panel B. (B2–B4) Representative PACAP-ir fibers with varicosities (*en passant* type) indicated by black arrows. (C) Horizontal section from a Prkcd-Cre::Ai9 mouse showing tdTomato-labeled PKCδ+ neurons (red) and PACAP immunostaining (green) in the CeC. (C1) Higher magnification of the caudal CeC reveals abundant PACAP-ir perisomatic rings around PKCδ+ cells, mainly located in the posterolateral portion of this horizontal plane. (D) High-resolution immunofluorescence for PACAP (blue), GluD1 (green), and PKCδ–Ai9–tdTomato (red) highlights PACAP-ir labeling around PKCδ+ somata, with GluD1 signals localized to membrane regions in close apposition to PACAP+ elements.

Electrophysiological analysis of PACAP-driven responses. In order to determine the postsynaptic response of PKCd-expressing neurons in the CeC to PACAP, we performed *ex vivo* whole-cell patch-clamp recordings in brain slices from Prkcd-Cre::Ai9 mice, in which PKCd+ neurons are labeled with TdTomato. Recordings were conducted in artificial cerebrospinal fluid (ACSF) with a 100 nM PACAP bath application followed by a washout period (Fig. 2A).

We report that whole-cell patch-clamp recordings from PKCδ+ neurons reveal two functionally distinct subtypes. Type 1 neurons show a robust and reversible increase in firing rate during PACAP application, along with a steeper current–frequency (I–F) relationship, while type 2 neurons exhibit no significant change in excitability. Figure 2, panels A–C show the type 1 neurons (red symbols) that exhibited a robust and reversible increase in action potential firing frequency during PACAP application (Fig. 2B), accompanied by an enhanced slope in the current–frequency (I–F) curve (Fig. 2C), which indicates increased intrinsic excitability. A two-way ANOVA revealed significant main effects of treatment, $F(2,780) = 25.64$, $p < 0.001$, and current injection steps, $F(12,780) = 298$, $p < 0.001$, with no significant interaction between the factors. *Post hoc* multiple comparisons confirmed a significant increase in excitability during PACAP application relative to baseline ($p < 0.001$), with firing rates returning to baseline levels during the washout (no significant difference compared to ACSF condition). Furthermore, *post hoc* immunohistochemistry demonstrated that these PACAP-responsive neurons expressed GluD1 at the plasma membrane (Fig. 2D, left panel), and their morphology was confirmed by biocytin filling (Fig. 2D, right panel). These characteristics are consistent with the perisomatically innervated PKCδ+ neurons described in Figure 1.

In contrast, type 2 neurons (blue symbols; Fig. 2E–F) showed no significant change in firing frequency during PACAP application. The two-way ANOVA for Type 2 neurons revealed a significant effect of current injection steps, $F(12,312) = 84.1$, $p < 0.001$, but no significant effect of treatment, $F(2,312) = 0.606$, $p > 0.05$, nor any significant interaction between the factors. Post hoc analysis confirmed no differences in firing rate under ACSF, during PACAP application, or during the washout period. Additionally, these PACAP-insensitive neurons lacked membrane-localized GluD1 despite being TdTomato-positive

(Fig. 2F, left panel), and their morphology was similarly confirmed via biocytin labeling (Fig. 2F, right panel).

Together, these findings support the existence of functionally and molecularly distinct subtypes of PKCδ+ neurons in the capsular division of the central amygdala, characterized by differential PACAP sensitivity and selective GluD1 expression.

Post hoc immunohistochemical analysis of these PACAP-sensitive cells revealed plasma membrane expression of GluD1 (Fig. 2D, left panel), and their cellular morphology was confirmed through biocytin filling (Fig. 2D, right panel). These features are consistent with the PKCδ+ neurons perisomatically innervated by the PACAP containing calyceal axons described in Figure 1. In contrast, type 2 neurons (blue symbols, Fig. 2E–F) exhibited no significant change in firing frequency during PACAP application. These PACAP-insensitive neurons lacked GluD1 membrane localization, despite also being tdTomato+ (Fig. 2F). Their identity and morphology were likewise confirmed via biocytin labeling (Fig. 2F, right panel).

These results support the existence of functionally and molecularly distinct subtypes of PKCδ+ neurons in the CeC, with differential sensitivity to PACAP and selective expression of GluD1.

Figure 2. Whole-cell patch-clamp recordings reveal both PACAP-sensitive and PACAP-insensitive subtypes of PKCδ+ neurons in the central amygdala (CeA). (A) Schematic of *ex vivo* recordings performed on horizontal brain slices from Prkcd-Cre::Ai9 mice, illustrating TdTomato-labeled PKCδ+ neurons in the capsular division of the CeA (CeC) red crosses symbolize the type 1 PKCδ+ cells, while the grey circles symbolized the type 2 PKCδ+ (*vide infra*). (B) Representative current-clamp traces from a PACAP-sensitive (type 1) neuron showing increased firing in response to 100 nM PACAP (red), which returns to baseline after washout (blue). (C) Current–frequency (I–F) curves demonstrating enhanced excitability of Type 1 neurons during PACAP application (red curve, n = 21). (D) Example of a type 1 cell with post hoc immunofluorescence that confirms GluD1 expression (cyan) localized to its plasma membrane (left) and biocytin labeling and its dendritic morphology and axonal projection (right). (E) In contrast, PACAP-insensitive (type 2) neurons (blue crosses, n=9) show no change in firing frequency following PACAP application. (F) Post hoc analysis of these Type 2 cells reveals the absence of GluD1 membrane expression (left) despite successful biocytin filling (right). Scale bars: 10 μm.

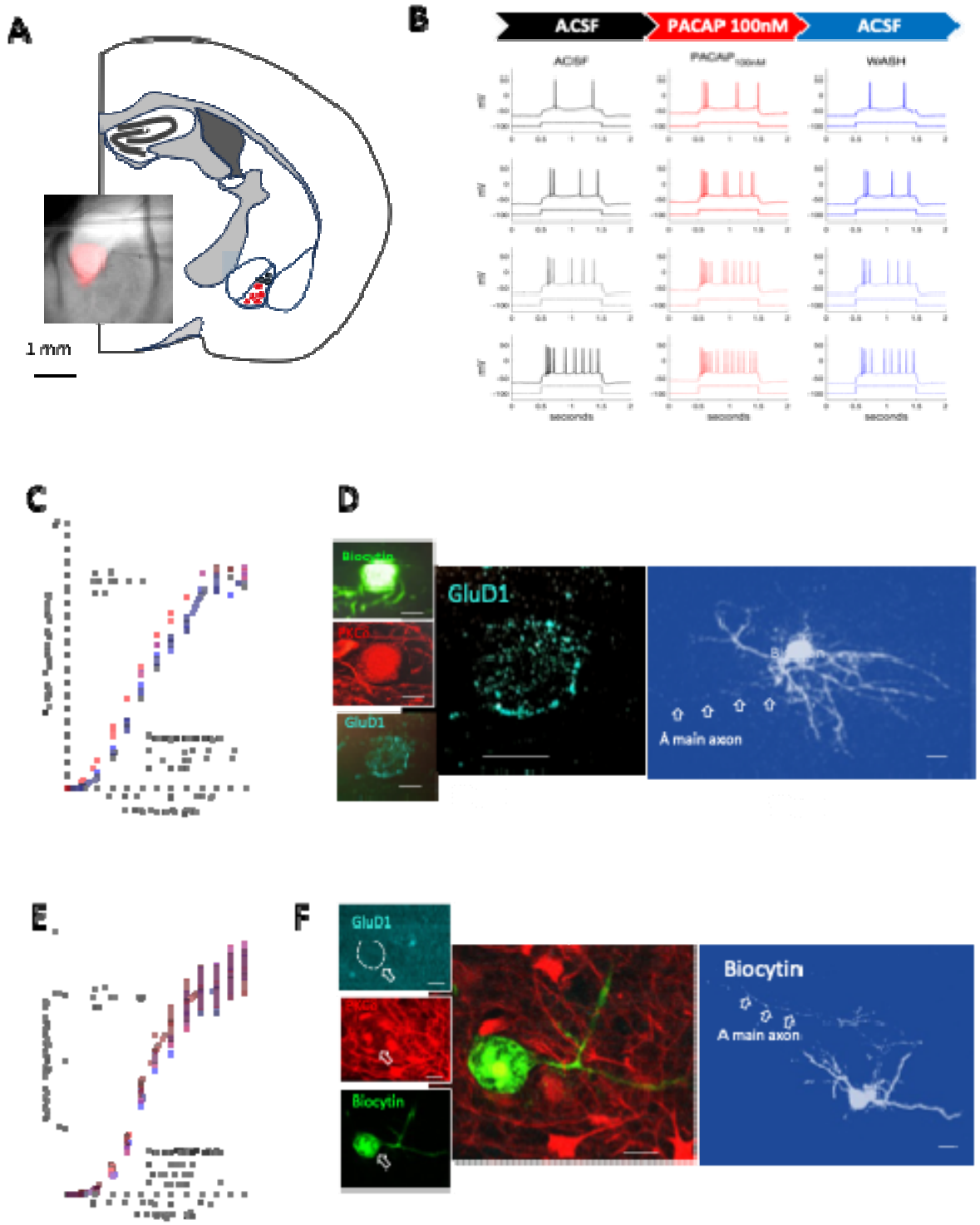

Figure 2 (caption in the previous page)

Molecular signature of calyceal terminals engulfing the PKCd-ir neurons in CeC. We then decided to delve further into the molecular architecture of these large perisomatic PACAP+ terminals. High-resolution confocal imaging revealed that these ring-like axon terminals co-expressed the vesicular glutamate transporter 1 (VGluT1) and/or 2 (VGluT2) (Fig. 3, panel D, A11, 12, A17, B6 y B7 and Fig. 5 panel H, at electron microscopy level), analogously to the calyx of Held in the medial nucleus of trapezoid body (MNTB), and the vesicular acetylcholine transporter VAChT (Fig. 3, panels B). Furthermore, the presynaptic PACAP+ rings around the somata of PKCd-expressing neurons contained the neuropeptides calcitonin-gene related peptide (CGRP) and neurotensin (NTs), as well as the calcium binding protein calretinin (Fig. 3, panels C). These findings indicate a multimodal transmitter phenotype for these axon terminals that include glutamatergic, cholinergic, and peptidergic components. To prove that their spatial organization is similar to that of a calyx of Held (calyx-like), we performed confocal z-stacks of PKCd-expressing neurons segmentation in the CeC. The PACAP+ fibers formed large cup-like, enveloping axo-somatic terminals, confirming their calyx-like macro-architecture (Fig. 3, D).

Figure 3: Neurochemical composition of the ring-like structure in the CeC: A. B: High-magnification confocal views demonstrate that these perisomatic structures co-express multiple markers, including in A: VGluT1 (green labeling), calretinin (red labeling), PACAP (white labeling) and PKCd (pink labeling); B: neurotensin (NTs, white labeling), vesicular acetylcholine transporter (VAChT, green labeling), VGluT2 (cyan labeling), and calcitonin gene-related peptide (CGRP red labeling). C: top row, co-expression of neuropeptides NTs (blue), PACAP (red) and calcium binding protein calretinin forming ring-like structure. Note that some targeted neurons are calretinin expressing (*). In one case, NTs/PACAP/calretinin co-expressed axon approached the targeted cell guided by its main dendrite (arrows at the top part of the for panels). Bottom row: co-expression of ring structure with PACAP/CGRP engulfing a PKCd expressing neurons. D. Segmentation of 20 serial confocal optical sections of two PKCd-expressing neurons of rat CeC (blue) illustrates the spatial organization of two VGluT1, VGluT2, PACAP co-expressing ring-like fibers surrounded their somata. Scale bars: 20µm.

(Figure 3 displayed in next page)

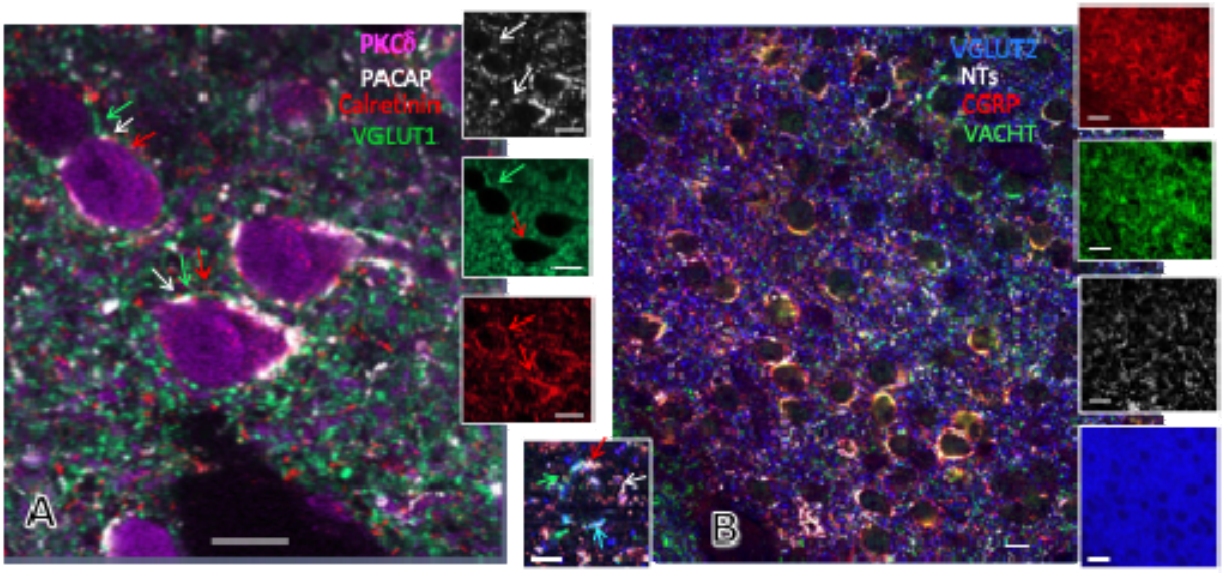
PKCδ
PACAP
Calretinin
VGLUT1
A
VGLUT2
NTs
CGRP
VACHT
B

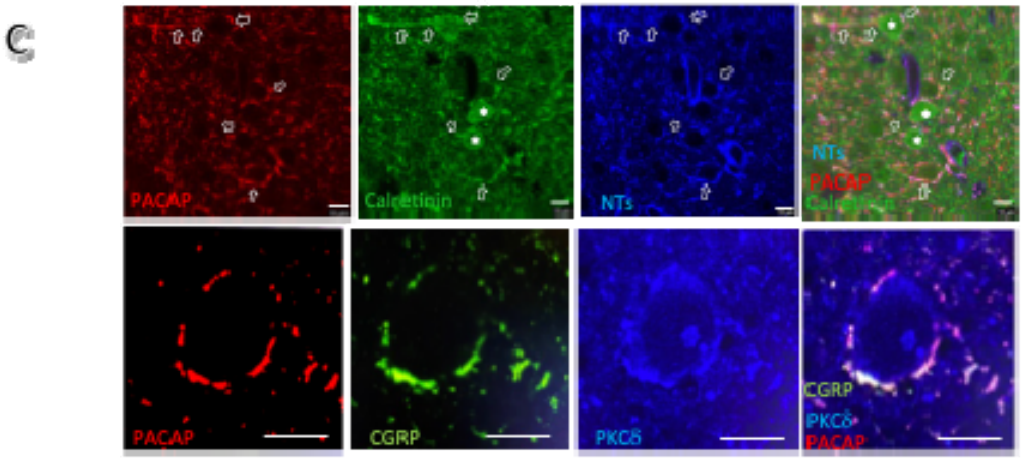
C
PACAP
Calretinin
NTs
NTs
PACAP
PACAP
CGRP
PKCδ
CGRP
PKCδ
PACAP

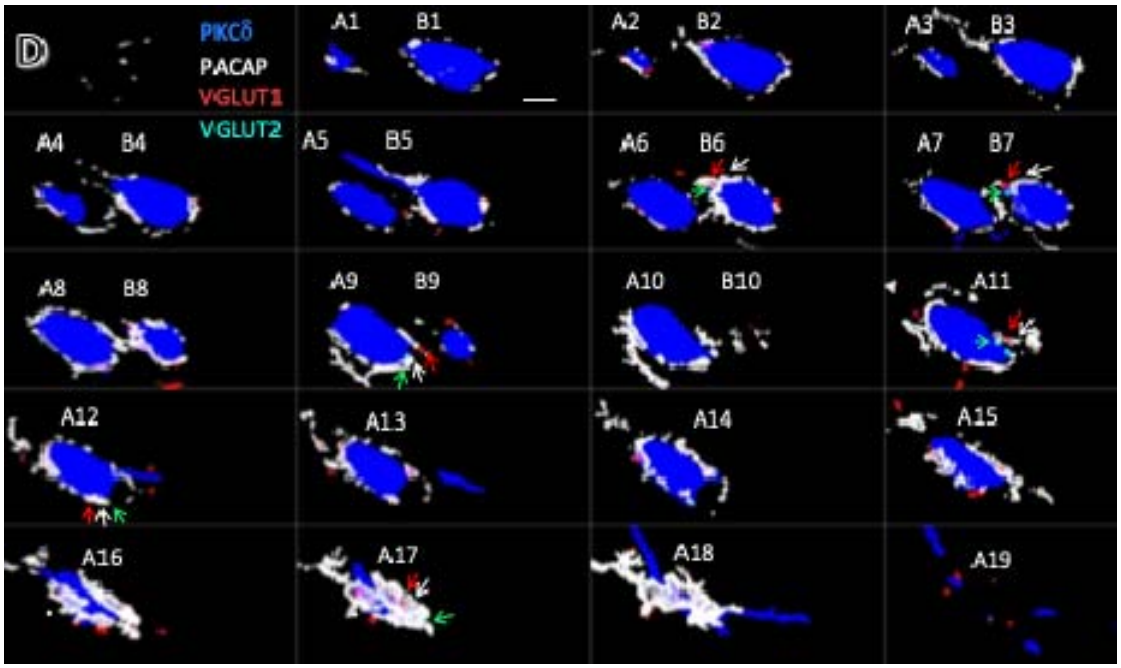
D
PKCδ
PACAP
VGLUT1
VGLUT2
A1 B1
A2 B2
A3 B3
A4 B4
A5 B5
A6 B6
A7 B7
A8 B8
A9 B9
A10 B10
A11
A12
A13
A14
A15
A16
A17
A18
A19

FIB-SEM and immunoelectron microscopy revealed the ultrastructural organization of PACAP+ ring structure is a giant, enveloping synapse with mixed synaptic specializations, including both asymmetric and symmetric synaptic contacts. To study the ultrastructural organization of these PACAP+ calyx-like structures, we employed focused ion beam-scanning electron microscopy (FIB-SEM, Crossbeam 550, Karl ZEISS Microscopy) combined with immunoelectron labeling. Analysis of two sets of serial sections (n = 450 and 240) from a DAB-labeled sample of the rat CeC revealed giant PACAP+ terminals engulfing the postsynaptic somata and exhibiting a dense network of synaptic contacts, fully consistent with a calyx of Held-like morphology (Fig. 4 and supplementary videos 1-3).

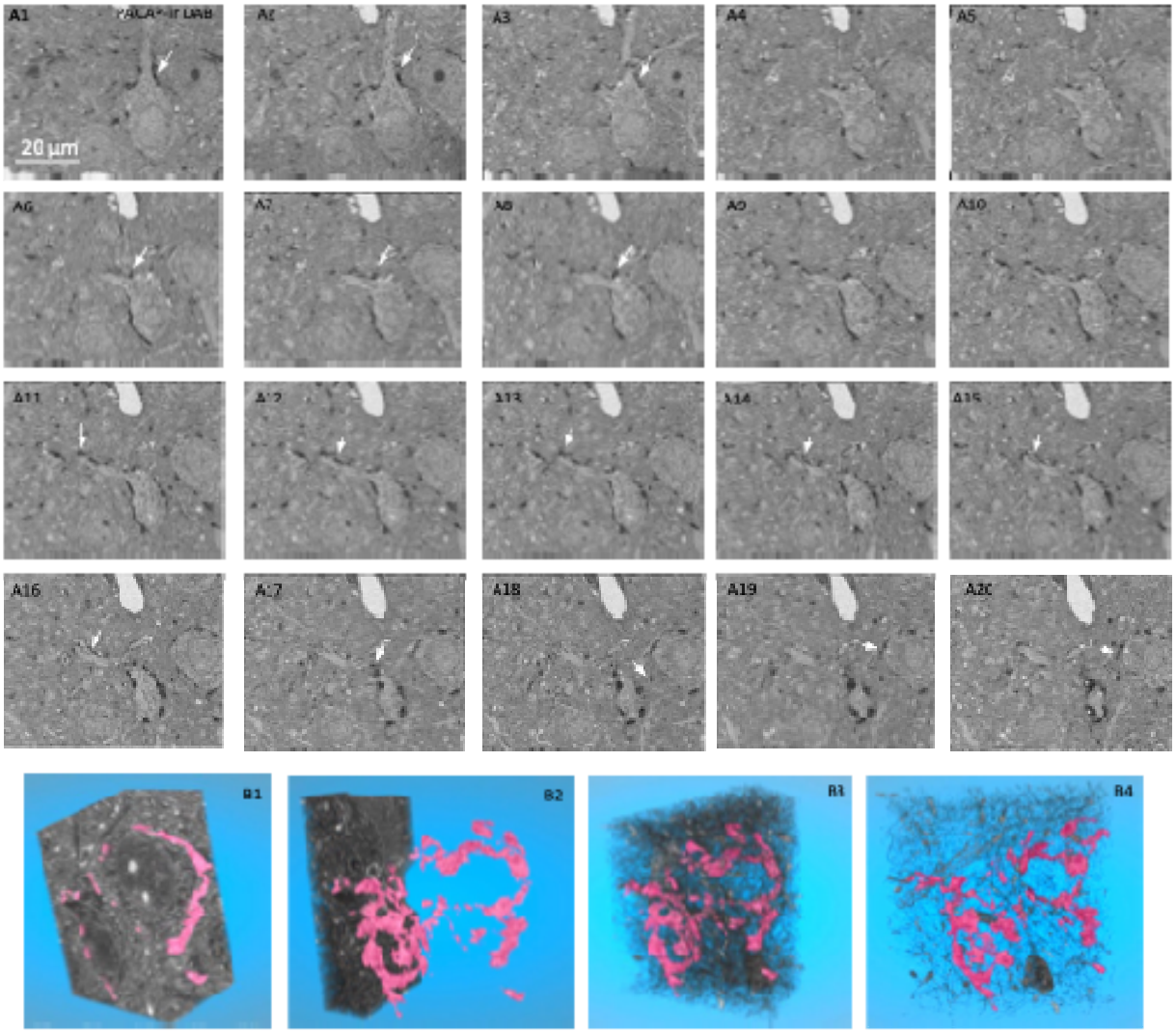

Figure 4. A calyx of Held-like, ring-shaped synaptic structure in the central amygdala (CeC-calyceal synapse) revealed by tomographic electron microscopy. Panels A1–A18: Selected frames from a series of 450 FIB-SEM (Focused Ion Beam Scanning Electron Microscopy) images from an immunoelectron microscopy sample labeled with rabbit anti-PACAP antibody and visualized using a peroxidase-DAB reaction. These frames illustrate the sequential progression of two PACAP-positive calyceal synapses. Panels B1–B4: 3D reconstruction and segmentation of the same sample highlighting the ring-like morphology of the PACAP+ calyceal synapses. Corresponding video files showing the full reconstruction are available in the Supplemental Information videos 1, 2 and 3.

Finally, by leveraging pre-embedding electron microscopy, we revealed that CeC calyx-like synapses exhibit unconventional chemo-anatomical properties. PACAP+ calyceal

axons formed both asymmetric (type I) and symmetric (type II) synaptic contacts (Fig. 5A), occasionally observed adjacent within the same terminal, but with a higher prevalence of type II configurations (Fig. 5B). Noteworthy, we often detected strong GluD1 immunometal labeling of the plasma membrane specialization of PKCd-expressing neurons postsynaptic to the PACAP+ terminals (Fig. 5C), suggesting a specific molecular identity for this synaptic pairing. Cholinergic terminals expressing VAChT also formed GluD1-positive type II synapses (Fig. 5D), reinforcing the idea that GluD1 expression is closely associated with cholinergic inputs. In contrast, nearby glutamatergic synapses (VGluT1/2-positive) typically exhibited classic asymmetric morphology and lacked GluD1 labeling (Fig. 5E). These findings support the notion that CeC-calyceal synapses represent a specialized subpopulation of central amygdalar connections, distinguished by their molecular profiles and potential neurotransmitter signaling mechanisms.

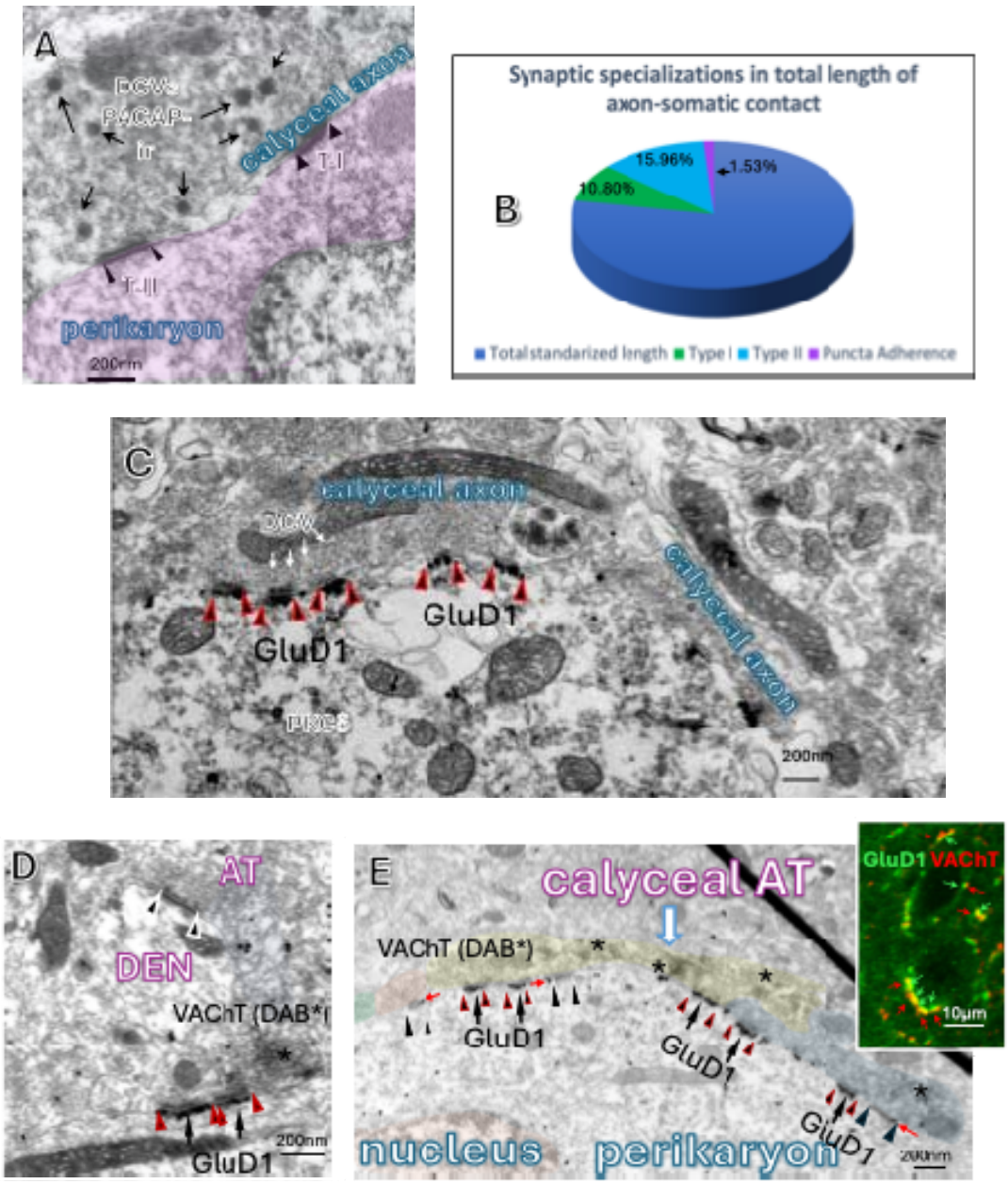

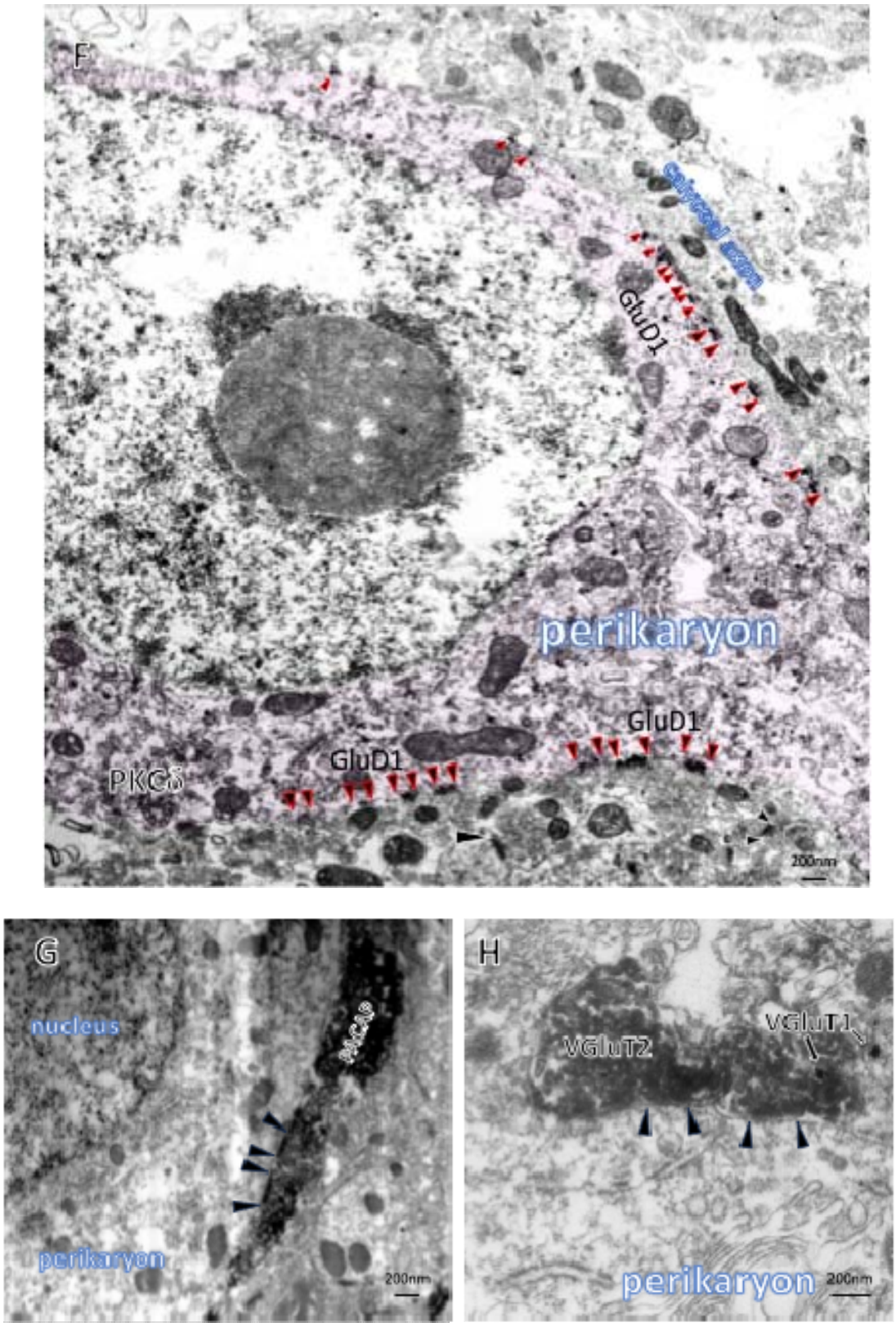
F
GluD1
perikaryon
GluD1
GluD1
PKCδ
200nm
G
nucleus
PKCAb
perikaryon
200nm
H
VGluT2
VGluT1
perikaryon
200nm

Figure 5. The CeC-calyceal synapse exhibits distinct chemoanatomical features.

A. A PACAP-expressing calyceal axon forms both asymmetric (type I, thick arrowheads) and symmetric (type II, narrow arrowheads) synaptic contacts. Presynaptic vesicles and both pre- and postsynaptic densities (PSDs) are visible. Arrows indicate PACAP+ dense core vesicles.

B. A pie chart quantifies the proportion of each synapse type based on contact length measurements from randomly selected TEM micrographs (n = 30) in which synaptic specializations could be identified.

C. Double-label immunoelectron microscopy (DAB for PKCδ and immunogold for GluD1) shows a PACAP+ calyceal axon making multiple type II synapses onto a PKCδ-expressing (DAB-labeled) neuron. The PSDs are densely labeled with GluD1-immunogold particles (red-black bicolored arrowheads).

D. A DAB-labeled axon terminal expressing vesicular acetylcholine transporter (VAChT, *) forms a type II synapse, with dense GluD1-gold particle labeling at the PSD (red-black arrowheads). For comparison, an adjacent unlabeled axon terminal (AT) forms a clear type I synapse devoid of GluD1 labeling (white-black arrowheads).

E. Another example of a VAChT+ (*) calyceal axon forming Type II synapses with GluD1-gold labeling (black arrows) at the PSDs. Inset: confocal image showing close spatial correspondence between VAChT (red) and GluD1 (green) signals. GluD1 expression is localized between the red VAChT-positive axon and the soma, suggesting a tight anatomo-functional association between cholinergic input and GluD1 expression.

F. A large PKCδ-expressing (DAB-labeled) neuron receives multiple GluD1-positive synaptic contacts (red-black arrowheads) along its soma and proximal dendrite. Two adjacent type I synapses from unlabeled axons are GluD1-negative (white-black arrowheads), underscoring the specificity of GluD1 labeling to type II synapses and suggesting a molecular distinction between glutamatergic and cholinergic inputs.

G. and **H** PACAP+ (panel G) and VGluT1 and VGluT2 co-expressing calyceal axon (panel H) form multiple synaptic specifications one contacts onto CeC cells.

Scale bars: 200nm.

Discussion

The extended amygdala (EA) is a specialized region of the striatum that projects to visceral centers in the brainstem (Swanson and Petrovich 1998). It receives inputs from prefrontal, insular, temporal and olfactory cortical areas, as well as from almost all other parts of the amygdala, from brainstem viscerosensory and nociceptive centers, and from parts of the caudal thalamus transmitting auditory and somatosensory information (Swanson and Petrovich 1998). Functions of EA include induction of visceromotor adjustment to emotional and behavioral situations, as well as processing of information necessary for the manifestation of emotional states such as fear and anxiety (Shackman and Fox 2016). In this study, we identified a multi-transmitter architecture of the calyceal synapse in the EA, that reveals a great degree of neurotransmitter convergence in a single structurally specialized terminal. These giant "cup-like" presynaptic endings co-express markers for glutamate (VGluT1/2), acetylcholine (VAChT), and multiple neuropeptides (PACAP, CGRP, and neurotensin), indicating a multi-transmitter phenotype unlike any previously described forebrain synapse. Extensive EM analysis revealed multiple asymmetric and symmetric synaptic specializations, often aligned with GluD1-immunolabeled postsynaptic domains. Electrophysiological recordings confirmed that PACAP application enhances excitability in CeC PKCδ/GluD1 expressing neurons, suggesting functional engagement of this novel synapse. Collectively, our findings uncover a previously unknown calyceal synapse in the forebrain, exhibiting a unique convergence of fast and modulatory transmission, with implications for the structural logic of high-fidelity signal integration in viscerosensory-affective circuits.

Co-transmission, the ability of one neuron to release several neurotransmitters – is now recognized as a general principle of neural communication (Granger, Wallace et al. 2017, Svensson, Apergis-Schoute et al. 2018, Wallace and Sabatini 2023). Classic examples range from peripheral autonomic junctions (e.g. the splanchnic nerve, a major component of the sympathetic nervous system, and PACAP are both release to post-synaptic chromaffin cells in the adrenal medulla in the stress response (Stroth, Kuri et al. 2013, Eiden, Emery et al. 2018); parasympathetic neurons co-releasing ACh with ATP and VIP to primary sensory afferents co-packaging glutamate with substance P and CGRP (Hokfelt, Pernow et al. 2001). In the CNS, co-transmission is often seen in modulatory circuits or developmental contexts, such as cholinergic basal forebrain neurons and habenular neurons that can co-release glutamate alongside ACh (Allen, Abogadie et al. 2006). However, the convergence of three or more signaling molecules in one giant presynaptic terminal, as observed here, is extraordinary and expands our understanding of synaptic diversity in forebrain circuits.

The identification of calyx-like terminals in the CeC and ovBST challenges traditional views of synaptic architecture in the extended amygdala and probably beyond. While calyceal synapses such as the calyx of Held are well characterized in auditory brainstem circuits for their fast, high-fidelity transmission, analogous structures have not previously been described in forebrain regions. The morphology and complexity of the terminals we observed—combined with their molecular signatures—suggest a similar capacity for rapid and synchronized signal delivery, potentially coordinating responses to highly salient visceral or emotional stimuli. Importantly, our findings indicate that the CeC calyx is not a "one-trick" fast excitatory synapse, but rather a multiplexed signaling hub. The presence of glutamatergic machinery (VGluT1/2) implies it can drive rapid, ionotropic excitation of its postsynaptic target, ensuring immediate spike transmission. In parallel, the cholinergic

component (VAChT+) could engage nicotinic receptors for additional fast depolarization or muscarinic receptors for slower, metabotropic modulation on the same postsynaptic neuron. The co-packaged neuropeptides (PACAP, CGRP, neurotensin) likely act on GPCRs to produce even longer-lasting effects – from second-messenger cascades that modulate ion channel excitability to gene expression changes that alter the neuron's state. In a structurally large synapse that envelopes the postsynaptic soma, these multiple transmitters can be released in a spatially and temporally coordinated manner, effectively “bombarding” the postsynaptic neuron with concurrent fast and slow signals. This arrangement may ensure that when the presynaptic neuron fires, it not only triggers an immediate action potential in the postsynaptic cell, but also sets the tone for that cell’s excitability and plasticity over seconds to minutes via cholinergic and peptidergic pathways. In essence, the calyceal synapse acts as a singular multimodal input capable of orchestrating both phasic and modulatory influences on its target.

The postsynaptic targets of these calyceal terminals are a distinct subset of PKCδ-positive (PKCδ$^+$) neurons in the central extended amygdala (CeC). In line with our observations, Torruella-Suárez et al. (2020) reported that NTs$^+$ fibers form perisomatic arrangements around a subset of PKCδ neurons in the central amygdala (see(Torruella-Suarez, Vandenberg et al. 2020) Fig. 1D), while other set of PKCδ cells appear to not be innervated. Although the authors did not explicitly discuss the functional implications of this heterogeneity, this finding aligns with our data suggesting that distinct NTs$^+$ inputs may confer differential modulatory influences on PKCδ neurons. This finding is intriguing given that PKCδ$^+$ neurons in the CeA are well-known modulators of emotional behavior: they have been identified as so-called “fear-off” neurons in the lateral CeA microcircuit, which inhibit the medial CeA output cells and thereby gate the expression of fear and defensive reactions (Hevesi, Zelena et al. 2021). Specifically, PKCδ$^+$ neurons (largely residing in the lateral/capsular CeA) tonically suppress downstream effectors of threat responses; when they fire, they can prevent excessive freezing or autonomic output by silencing the CeM output neurons (Hevesi, Zelena et al. 2021). Our data now position these PKCδ$^+$ cells as recipients of a potent multimodal excitatory drive. This raises the question: How might the convergence of fast excitatory and modulatory transmitters at one synapse influence CeA microcircuit function and emotional behavior?

A key consequence of the calyceal input is likely a strong and immediate depolarization of PKCδ$^+$ neurons via glutamatergic AMPA/NMDA receptor activation – effectively a reliable trigger to make these inhibitory neurons fire spikes with minimal delay. The large number of active zones observed in the calyx EM reconstructions (Fig. 4) and the presumably high release probability (by analogy to the calyx of Held) suggest that each presynaptic action potential can generate a near-synchronous EPSP in the PKCδ$^+$ neuron. This fast excitation would rapidly recruit the PKCδ$^+$ cell into the circuit, causing it to release GABA onto its targets (including CeM output neurons). In the context of a threatening or salient stimulus, such an arrangement could provide an “all hands on deck” signal to the PKCδ$^+$ neuron: not only does it receive a swift excitatory drive, but concurrently the ACh and neuropeptides released from the same terminal may modulate its responsiveness and downstream effects. Acetylcholine, for instance, could activate postsynaptic muscarinic receptors on the PKCδ$^+$ neuron, which often induce a slow depolarization or reduce potassium conductance, thereby prolonging the excitatory effect of the initial glutamatergic EPSP. This might keep the PKCδ$^+$ neuron firing for an extended period even after the presynaptic burst ends, sustaining the inhibitory influence on CeM output. In parallel, neuropeptides like PACAP and CGRP can engage their GPCRs (PAC_1 and CGRP

receptors, respectively) on the PKCδ$^+$ neuron. PACAP in particular is known for triggering cAMP/PKA signaling cascades that greatly enhance neuronal excitability and induce transcriptional changes related to plasticity (Meloni, Kaye et al. 2019). Thus, a strong burst of activity in the presynaptic calyceal fiber could not only cause immediate inhibition of CeM via PKCδ$^+$ activation, but also prime the PKCδ$^+$ neuron for longer-lasting changes – for example, upregulating activity-regulated genes, like Arc/Arg3.1, which PACAP is known to increase in CeA neurons (Meloni, Kaye et al. 2019) or strengthening specific synapses through plasticity on vesicular transporters expression (Zhang, Hernandez et al. 2021). In short, the combination of fast glutamatergic drive with ACh and peptide co-transmission means this synapse can simultaneously function in the rapid execution of a circuit response and in the modulation of that circuit's sensitivity over time. Such dual capability is especially significant in the extended amygdala, where acute reactions and longer-term mood states are tightly interconnected.

From a systems perspective, this calyceal synapse represents a node of convergence between viscerosensory inputs and emotional processing. The extended amygdala is thought to integrate signals from the body (pain, discomfort, visceral threat) with limbic information to orchestrate appropriate behavioral and physiological responses. Our findings align with emerging evidence that specific brainstem-derived inputs carry visceral threat signals into the CeA. Notably, the lateral parabrachial nucleus (PBN) provides a major glutamatergic projection to the CeC and is a known source of CGRP- and PACAP-positive fibers that target PKCδ$^+$ neurons (Jiang, Zhang et al. 2023).

The physiological relevance of this synaptic architecture likely lies in its ability to tightly couple immediate sensory input with modulatory context. Our findings align with recent work which demonstrated that high-fidelity parabrachial inputs to the lateral central amygdala reliably induce Fos expression in response to hypotension, underscoring the pathway's critical role in cardiovascular regulation (Takeuchi, Xie et al. 2004).

In summary, the identification of a multi-transmitter, calyceal-like synapse in the extended amygdala underscores the principle that synaptic structure and chemistry are tuned to circuit function. This giant axo-somatic synapse provides a high-impact input onto CeA PKCδ$^+$ neurons, allowing a single presynaptic action potential to deliver a multifaceted message: an immediate jolt of excitation together with a bouquet of modulators that shape the ensuing neuronal and network response. This design may ensure that salient visceral threats (e.g., cardiovascular dysregulation, intense pain or other internal danger signals) are met with an equally complex and robust response in the integrative nodes of the emotional brain. By expanding the repertoire of known synapse types in the forebrain, our findings prompt a reexamination of how diversity in synaptic form and transmitter content contributes to behavioral outcomes. The extended amygdala, long recognized as a hub for emotional-autonomic integration, now can be seen to house specialized synapses that literally connect the "gut feeling" to the generation of adaptive (or maladaptive) emotional states. Elucidating the regulation and plasticity of these calyceal synapses will be an exciting direction for future research, one that may bridge the gap from molecules and microcircuits to the complex phenomena of stress, emotion, and somatic experience in health and disease.

Technical consideration. Our data reveal that the presynaptic compartments of these calyx-like terminals in the CeC are enriched in multiple neurotransmitter markers, including VGluT1, VGluT2, VAChT, PACAP, neurotensin (NT), and CGRP. The multichannel

immunofluorescence confocal images strongly suggest that these markers are present within the overall calyceal structure. However, it is important to note that the spatial resolution of confocal microscopy and the inherent limitations of immunohistochemical labeling—which only targets the antigen and not the membrane—do not allow us to conclusively determine whether all of these transmitters are expressed within the same individual axon or whether they derive from distinct axonal sources converging at the same synaptic site. This ambiguity is underscored by our Supplemental Figure 2, where combined immunogold (for VGluT1) and immunoperoxidase (for PACAP) labeling illustrates that, although a proximal dendritic segment receives inputs from calyceal-type axons with differing chemical signatures, the method does not provide a definitive univocal assignment of all markers to a single presynaptic element.

Moreover, while immunogold electron microscopy combined with immunoperoxidase labeling offers enhanced resolution, this technique is technically limited to the simultaneous detection of only two antigens per reaction. Thus, although our current data highlight a multimodal transmitter phenotype at these synapses, further studies employing advanced multiplexed ultrastructural techniques will be necessary to definitively elucidate whether these diverse neurotransmitter systems are co-localized within the same axon or represent a convergence of multiple inputs. For instance, tomographic EM combined with multiple immunogold labels as well as viral vector tracked tracing form idented upstream input region(s). Overall, these findings underscore the functional complexity of synaptic integration within the extended amygdala, suggesting that even highly specialized structures such as calyx-like terminals might employ a multifaceted transmitter strategy to modulate postsynaptic activity.

Materials and methods

Rats.
Adult (>60 days) male Wistar rats were obtained from the vivarium of the School of Medicine, National Autonomous University of Mexico. Rats were housed under controlled temperature and humidity on a 12-h light cycle (lights on at 07:00, off at 19:00) with ad libitum access to standard chow and water. All procedures were approved by the School of Medicine's Ethics Committee (License: CIEFM-079-2020).

Mice.
PKCδ-Ai9-TdTomato mice were generated by crossing heterozygous Prkcd-Cre knock-in mice (Jackson Laboratory, stock #027857) with Ai9 Cre-dependent reporter mice (stock #007909); double-positive offspring were identified via PCR. In addition, adult male and female C57BL/6J wild-type and PKCδ-Ai9 animals were maintained under similar conditions. All procedures with mice were approved by the National Institute of Mental Health Animal Care and Use Committee (NIMH/ACUC approval LCMR-08).

Immunohistochemistry for light microscopy

Rodents were perfused via the ascending aorta with 0.9% NaCl followed by 4% paraformaldehyde. Brains were sectioned at 70 µm using a Leica VT1200 vibratome. Sections were washed in phosphate buffer (PB), blocked for 2 hours in TBST (0.05 M Tris, 0.9% NaCl, 0.3% Triton-X) plus 10% normal donkey serum, and incubated overnight at 4°C with primary antibodies (see SI table 1 diluted in TBST with 1% serum. After washing, sections were incubated for 2 hours at room temperature with appropriate biotinylated or

fluorescent secondary antibodies (1:500; Vector Laboratories). Brightfield images were acquired using a Nikon Eclipse E600, and confocal images were acquired with a Leica Stellaris microscope.

Ex Vivo whole-cell electrophysiology

Brain slices (300 µm thick) containing the central amygdala (CeA) were obtained from Ai9-TdTomato-PKCδ mice. Following rapid extraction, brains were placed in an ice-cold cutting solution (in mM: 92 NMDG, 20 HEPES, 25 glucose, 30 $NaHCO_3$, 2.5 KCl, 1.2 NaH_2PO_4, 10 $MgSO_4$, 0.5 $CaCl_2$; osmolarity 303–306 mOsm; 95% O_2/5% CO_2). Slices were cut with a Leica VT1200 and incubated at 34°C for 5 minutes, then maintained in holding aCSF (in mM: 92 NaCl, 20 HEPES, 25 glucose, 30 $NaHCO_3$, 2.5 KCl, 1.2 NaH_2PO_4, 1 $MgSO_4$, 2 $CaCl_2$) at room temperature for at least 1 hour. For current-clamp recordings, micropipettes (3–5 MΩ) were filled with an internal solution (in mM: 135 K-gluconate, 10 HEPES, 4 KCl, 4 Mg-ATP, 0.3 Na-GTP, 0.2% biocytin). Neurons were visualized using differential interference contrast (DIC) and identified by TdTomato fluorescence. PACAP (100 nM) was bath-applied during a current injection protocol (1 s steps from -40 to 240 pA in 20 pA increments, 7 s intervals), and data were analyzed using GraphPad Prism. Only cells with stable series resistance (<20 MΩ) were included.

Transmission Electron Microscopy

Brains from C57BL/6 mice were sectioned at 40 µm (Leica VT1000) and processed for immuno-EM. Sections were rinsed in PB, incubated in 1% sodium borohydride for 30 minutes, and blocked in a solution containing 1% normal goat serum and 4% bovine serum albumin in PB with 0.02% saponin. Primary antibodies (see SI table 1) were applied for 24 h at 4°C in blocking solution. After rinsing, sections were incubated overnight at 4°C with Nanogold-Fab' secondary antibodies (1:100) and processed using Vectastain ABC-HRP kits. Silver enhancement was performed with the HQ Silver Enhancement Kit (7 min at room temperature), followed by visualization of DAB reaction (0.025% DAB, 0.003% H_2O_2). Sections were post-fixed with 0.5% osmium tetroxide, stained with uranyl acetate, dehydrated through graded ethanol and propylene oxide, and flat embedded in Durcupan ACM epoxy resin. Ultrathin sections (~60 nm) were cut using a Leica Ultramicrotome UC7, collected on formvar-coated grids, counterstained with Reynolds lead citrate, and imaged using a Tecnai G2 12 transmission electron microscope with a OneView digital camera.

FIB-SEM Tomography

For three-dimensional reconstruction of calyx-like contacts, slices previously processed for PACAP immunolabeling were embedded in Durcupan resin and platinum-coated. A ZEISS Crossbeam 550 FIB-SEM was used. After milling a coarse trench with a 15 nA ion beam, a protective platinum layer (~1 µm thick) was deposited using the gas injection system at 30 kV/3 nA. A chevron-patterned registration mark was milled for alignment. Serial backscattered electron images were acquired using an accelerating voltage of 3 kV and a pixel size of 20 nm × 10 nm, with a slice thickness of 20 nm. The image stack was assembled into a volume and analyzed using ORS Dragonfly software.

Statistics

Data from electrophysiological recordings were analyzed by classifying neurons as PACAP responders (n = 21) or non-responders (n = 9) using a two-way ANOVA with treatment (baseline, PACAP, washout) and current step amplitude as factors. GraphPad Prism was used for statistical comparisons.

See supplemental Information (SI) for details of materials and method and a summary of primary and secondary antibodies, including dilutions, sources, and catalog numbers, in the SI Table

Acknowledgements

This research was supported by funding from the following sources: the National Autonomous University of Mexico (UNAM-PAPIIT-IG200121 to LZ and RAB); the Mexican Secretaría de Ciencia, Humanidad, Tecnología e Innovación (Secihti, CF-2023-G-243 to LZ, RAB, and RHP; CB-238744 to RAB); and the Intramural Research Program of the NIMH, NIH (ZIAMH002386 to LEE). The investigators were additionally supported by fellowships, including: a sabbatical year fellowship from the PASPA-DGAPA program (UNAM, to LZ and VSH); a Secihti sabbatical fellowship (to LZ); and a Fulbright-García Robles Fellowship (to VSH). We extend our deepest gratitude to Rafael Luján (UCLM, Spain), Luis Miguel García-Segura, Javier deFelipe, and Angel Merchán (Cajal Institute, Spain), Sebastian Schädler (Carl Zeiss Microscopy GmbH, Germany), and Claus Burkhart (NMI, Germany) for their invaluable guidance and support in FIB-SEM techniques. We also thank Marisela Morales for introducing us to the NIDA Confocal and Electron Microscopy Core. Finally, LZ wishes to express her profound gratitude to her mentor, Peter Somogyi, for hosting her 2019 summer research stay in Oxford, for his time spent examining raw materials under the microscope together with her, and for his insightful suggestion regarding the possibility of a Calyx of Held-like synapse.

References

Allen, T. G., F. C. Abogadie and D. A. Brown (2006). "Simultaneous release of glutamate and acetylcholine from single magnocellular "cholinergic" basal forebrain neurons." J Neurosci **26**(5): 1588-1595.
Botta, P., L. Demmou, Y. Kasugai, M. Markovic, C. Xu, J. P. Fadok, T. Lu, M. M. Poe, L. Xu, J. M. Cook, U. Rudolph, P. Sah, F. Ferraguti and A. Luthi (2015). "Regulating anxiety with extrasynaptic inhibition." Nat Neurosci **18**(10): 1493-1500.
Dai, J., C. Patzke, K. Liakath-Ali, E. Seigneur and T. C. Sudhof (2021). "GluD1 is a signal transduction device disguised as an ionotropic receptor." Nature **595**(7866): 261-265.
Daniel, S. E. and D. G. Rainnie (2016). "Stress Modulation of Opposing Circuits in the Bed Nucleus of the Stria Terminalis." Neuropsychopharmacology **41**(1): 103-125.
Dong, Y. L., Y. Fukazawa, W. Wang, N. Kamasawa and R. Shigemoto (2010). "Differential postsynaptic compartments in the laterocapsular division of the central nucleus of amygdala for afferents from the parabrachial nucleus and the basolateral nucleus in the rat." J Comp Neurol **518**(23): 4771-4791.
Eiden, L. E., A. C. Emery, L. Zhang and C. B. Smith (2018). "PACAP signaling in stress: insights from the chromaffin cell." Pflugers Arch **470**(1): 79-88.
Gandhi, P. J., D. Y. Gawande, G. P. Shelkar, S. G. Gakare, T. Kiritoshi, G. Ji, B. Misra, R. Pavuluri, J. Liu, V. Neugebauer and S. M. Dravid (2021). "Dysfunction of Glutamate Delta-1

Receptor-Cerebellin 1 Trans-Synaptic Signaling in the Central Amygdala in Chronic Pain." Cells **10**(10).
Goehler, L. (2011). Vicerosensory pathway in the brain. The science and clinical application of manual therapy. H. King, J. W and M. Patterson. Edinburgh, Churchill Livingston Elsevier**:** 163-179.
Granger, A. J., M. L. Wallace and B. L. Sabatini (2017). "Multi-transmitter neurons in the mammalian central nervous system." Curr Opin Neurobiol **45**: 85-91.
Harris, K. M. and R. J. Weinberg (2012). "Ultrastructure of synapses in the mammalian brain." Cold Spring Harb Perspect Biol **4**(5).
Held, H. (1893). "Die centrale Gehörleitung." Arch Anat Physiol Anat Abt,.
Hevesi, Z., D. Zelena, R. A. Romanov, J. Hanics, A. Ignacz, A. Zambon, D. D. Pollak, D. Lendvai, K. Schlett, M. Palkovits, T. Harkany, T. G. M. Hokfelt and A. Alpar (2021). "Secretagogin marks amygdaloid PKCdelta interneurons and modulates NMDA receptor availability." Proc Natl Acad Sci U S A **118**(7).
Hokfelt, T., B. Pernow and J. Wahren (2001). "Substance P: a pioneer amongst neuropeptides." J Intern Med **249**(1): 27-40.
Jaramillo, A. A., J. A. Brown and D. G. Winder (2021). "Danger and distress: Parabrachial-extended amygdala circuits." Neuropharmacology **198**: 108757.
Jiang, S. Z., H. Y. Zhang and L. E. Eiden (2023). "PACAP Controls Endocrine and Behavioral Stress Responses via Separate Brain Circuits." Biol Psychiatry Glob Open Sci **3**(4): 673-685.
Liakath-Ali, K., J. S. Polepalli, S. J. Lee, J. F. Cloutier and T. C. Sudhof (2022). "Transsynaptic cerebellin 4-neogenin 1 signaling mediates LTP in the mouse dentate gyrus." Proc Natl Acad Sci U S A **119**(20): e2123421119.
Lorteije, J. A., S. I. Rusu, C. Kushmerick and J. G. Borst (2009). "Reliability and precision of the mouse calyx of Held synapse." J Neurosci **29**(44): 13770-13784.
Meloni, E. G., K. T. Kaye, A. Venkataraman and W. A. Carlezon, Jr. (2019). "PACAP increases Arc/Arg 3.1 expression within the extended amygdala after fear conditioning in rats." Neurobiol Learn Mem **157**: 24-34.
Missig, G., C. W. Roman, M. A. Vizzard, K. M. Braas, S. E. Hammack and V. May (2014). "Parabrachial nucleus (PBn) pituitary adenylate cyclase activating polypeptide (PACAP) signaling in the amygdala: implication for the sensory and behavioral effects of pain." Neuropharmacology **86**: 38-48.
Nakamura, P. A. and K. S. Cramer (2011). "Formation and maturation of the calyx of Held." Hear Res **276**(1-2): 70-78.
Radke, A. K. (2009). "The role of the bed nucleus of the stria terminalis in learning to fear." J Neurosci **29**(49): 15351-15352.
Satzler, K., L. F. Sohl, J. H. Bollmann, J. G. Borst, M. Frotscher, B. Sakmann and J. H. Lubke (2002). "Three-dimensional reconstruction of a calyx of Held and its postsynaptic principal neuron in the medial nucleus of the trapezoid body." J Neurosci **22**(24): 10567-10579.
Schwaber, J. S., C. Sternini, N. C. Brecha, W. T. Rogers and J. P. Card (1988). "Neurons containing calcitonin gene-related peptide in the parabrachial nucleus project to the central nucleus of the amygdala." J Comp Neurol **270**(3): 416-426, 398-419.
Shackman, A. J. and A. S. Fox (2016). "Contributions of the Central Extended Amygdala to Fear and Anxiety." J Neurosci **36**(31): 8050-8063.
Shimada, S., S. Shiosaka, P. C. Emson, C. J. Hillyard, S. Girgis, I. MacIntyre and M. Tohyama (1985). "Calcitonin gene-related peptidergic projection from the parabrachial area to the forebrain and diencephalon in the rat: an immunohistochemical analysis." Neuroscience **16**(3): 607-616.

Stroth, N., B. A. Kuri, T. Mustafa, S. A. Chan, C. B. Smith and L. E. Eiden (2013). "PACAP controls adrenomedullary catecholamine secretion and expression of catecholamine biosynthetic enzymes at high splanchnic nerve firing rates characteristic of stress transduction in male mice." Endocrinology **154**(1): 330-339.
Svensson, E., J. Apergis-Schoute, G. Burnstock, M. P. Nusbaum, D. Parker and H. B. Schioth (2018). "General Principles of Neuronal Co-transmission: Insights From Multiple Model Systems." Front Neural Circuits **12**: 117.
Swanson, L. W. and G. D. Petrovich (1998). "What is the amygdala?" Trends Neurosci **21**(8): 323-331.
Takeuchi, Y., Q. Xie, T. Miki, Y. Matsumoto, I. Satriotomo, H. P. Li and H. Gu (2004). "Parabrachial inputs to Fos-immunoreactive neurons in the lateral central nucleus of amygdala activated by hypotension: a light and electron microscopic study in the rat." Brain Res Bull **64**(2): 171-180.
Torruella-Suarez, M. L., J. R. Vandenberg, E. S. Cogan, G. J. Tipton, A. Teklezghi, K. Dange, G. K. Patel, J. A. McHenry, J. A. Hardaway, P. A. Kantak, N. A. Crowley, J. F. DiBerto, S. P. Faccidomo, C. W. Hodge, G. D. Stuber and Z. A. McElligott (2020). "Manipulations of Central Amygdala Neurotensin Neurons Alter the Consumption of Ethanol and Sweet Fluids in Mice." J Neurosci **40**(3): 632-647.
Wallace, M. L. and B. L. Sabatini (2023). "Synaptic and circuit functions of multitransmitter neurons in the mammalian brain." Neuron **111**(19): 2969-2983.
Zhang, L., V. S. Hernandez, C. R. Gerfen, S. Z. Jiang, L. Zavala, R. A. Barrio and L. E. Eiden (2021). "Behavioral role of PACAP signaling reflects its selective distribution in glutamatergic and GABAergic neuronal subpopulations." Elife **10**.